ARTICLE
Journal of Cellular Biochemistry 110:219–228 (2010)

Journal of Cellular Biochemistry

Subcellular Proteome Analysis Unraveled Annexin A2 Related to Immune Liver Fibrosis

Lijun Zhang,[1*] Xia Peng,[1] Zhanqin Zhang,[1] Yanling Feng,[1] Xiaofang Jia,[1] Yuxin Shi,[1] Hua Yang,[1] Zhiyong Zhang,[1] Xiaonan Zhang,[1] Liwen Liu,[1] Lin Yin,[1] and Zhenghong Yuan[1,2**]

[1]*Shanghai Public Health Clinical Center, Shanghai 201508, China*

[2]*Key Laboratory of Molecular Virology, Shanghai Medical College, Fudan University, Shanghai 200032, China*

ABSTRACT

It is important to study the mechanism of liver fibrogenesis, and find new non-invasive biomarkers. In this study, we used subcellular proteomic technology to study the plasma membrane (PM) proteins related to immune liver fibrosis and search for new non-invasive biomarkers. A rat liver fibrosis model was induced by pig serum injection. The liver fibrogenesis from stage (S) S0-1, S2, S3-4, and S4 was detected by Masson staining and HE staining in this rat model after 2, 4, 6, and 8 weeks of treatment. The liver PM was enriched and analyzed using subcellular proteomic technology. The differentially expressed proteins were verified by Western blotting, immunohistochemistry, and ELISA. PM with 149-fold purification was obtained and 22 differentially expressed proteins were identified. Of which, annexin A2 (ANXA2) was detected to be increased obviously in S4 compared with S0-1, and verified by Western blotting of rat liver tissue and immunohistochemistry of rat and human liver tissue. The expression of ANXA2 in human plasma with S1-2 was also found to be up-regulated for 1.4-fold than that in S0. Furthermore, ANXA2 was detected to translocate from nuclear membrane and cytosol to PM as HBV stimulation through immunocytochemical analysis in vitro. This study identified 22 differentially expressed proteins related to liver fibrosis, and verified a potential biomarker (ANXA2) for non-invasive diagnosis of immune liver fibrosis. To our knowledge, it was the first time to dynamically study the proteins related to liver fibrosis and select biomarkers for liver fibrosis diagnosis through PM proteome research. J. Cell. Biochem. 110: 219–228, 2010.

KEY WORDS: LIVER FIBROSIS; PLASMA MEMBRANE; PROTEOMICS; ANXA2

Chronic infection with hepatitis B virus (HBV), persistently infecting more than 350 million individuals worldwide, often leads to progressive liver disease, including fibrosis, cirrhosis, and hepatocellular carcinoma [Pungpapong et al., 2007; Liaw, 2009]. Unfortunately, efforts to manage this growing public health problem have been hindered by vaccine failure in some individuals and the limited efficacy of current treatment modalities. These observations point to the importance of better understanding the molecular mechanisms for liver fibrosis caused by HBV. Numerous researches [Chisari and Ferrari, 1995; Wang et al., 2007] showed that the immune response to HBV-encoded antigens is responsible both for viral clearance and for liver pathology during HBV infection. Chronic hepatic injury stimulates and activates hepatic stellate cells (HSCs), which express α-smooth muscle actin (α-SMA), and other

Abbreviations used: ILF, immune liver fibrosis; 2-DE, two-dimensional gel electrophoresis; LC–MS, liquid chromatography–mass spectrometry; HCT, high capacity trap; HBV, hepatitis B virus; WB, Western blotting; HE, hematoxylin and eosin; ELISA, enzyme-linked immunosorbent assay; ANXA2, annexin A2; K8, keratin 8.

Lijun Zhang and Xia Peng contributed equally to this work.

Additional Supporting Information may be found in the online version of this article.

Grant sponsor: National 863 Project of China; Grant number: 2006AA02A411; Grant sponsor: Wang bao En Liver Fibrosis of China Liver Disease; Grant number: 20070026; Grant sponsor: Shanghai Natural Science Foundation; Grant number: 09ZR1426300; Grant sponsor: Research Foundation for Talented Scholars by Shanghai Public Clinical Center; Grant number: RCJJP2; Grant sponsor: Research Foundation (Shanghai Scientific and Technological Commission); Grant number: 09411965800.

*Correspondence to: Lijun Zhang, Scientific Research Center, Public Health Clinical Center, Shanghai 201508, China. E-mail: zhanglijun1221@163.com

**Correspondence to: Zhenghong Yuan, Key Laboratory of Molecular Virology, Shanghai Medical College, Fudan University, Shanghai 200032, China. E-mail: zhyuan@shaphc.org

Received 12 July 2009; Accepted 12 January 2010 • DOI 10.1002/jcb.22529 • © 2010 Wiley-Liss, Inc.

Published online 11 March 2010 in Wiley InterScience (www.interscience.wiley.com).

extracellular matrix (ECM) proteins [Benyon and Iredale, 2000]. Many biomarkers were found including class I biomarkers of liver fibrosis such as prolyl hydroxylase, monoamine oxidase, lysyl oxidase, type I, III, IV, and VI-procollagen, laminin, undulin, and so on, and class II biomarkers such as PGAA-index, Actitest, Fibrotest, and so on [Gressner et al., 2007]. As reviewed by Thomas A Wynn [2007], fibrosis is often defined as a wound-healing response that has gone out of control. In this progress, cells was wounded and healed, many proteins were involved such as α-SMA, fibrotest, and so on. However, so far, little is known about cell surface proteins that take part in fibrosis development and how HBV affected these proteins.

Proteomics has been widely used in the study of liver fibrosis [Spano et al., 2008; Smyth et al., 2009]. Recent advances in proteomic strategies and tools enable multiple fractionation, multiple protein identifications, and parallel analyses of multiple samples. However, low copy proteins were usually lost in whole cell or tissue. So recently, many proteomic investigations have focused on subcellular compartments [Liu et al., 2008]. The plasma membrane (PM) is an organized system serving as a structural and communication interface for exchanges of information and substances with the extracellular environment. The proteins on the PM act as ''doorbells'' and ''doorways'' playing crucial roles in cell function, including intercellular communication, cellular development, cell migration, and drug resistance [Pedersen et al., 2003; Mannova et al., 2006; Pizarro-Cerda and Cossart, 2006; de Laurentiis et al., 2007]. Therefore, it is important to study the PM proteins involved in liver fibrosis. However, due to unavailable models mimicking liver fibrogenesis caused by HBV infection, the research was greatly hindered. Immune hepatic fibrosis models [Tsukamoto et al., 1990; Schuppan et al., 2001; Baba et al., 2004], which mimic chronic hepatic injury caused by HBV, were widely used to research liver fibrosis. Of these immune hepatic fibrosis models, pig serum (PS)-induced rat hepatic fibrosis [Tsukamoto et al., 1990; Baba et al., 2004] was mostly used in the study of liver fibrosis. Histologically, the changes in this model were characterized by mononuclear cell infiltration and fibrotic response in the periportal area, followed by the septum formation connecting portal tract with central veins without hepatocyte injury [Tsukamoto et al., 1990]. This model has attracted more and more interest [Baba et al., 2005; Fujisawa et al., 2006] for it resembles the human disease and can serve as a suitable animal model for studying human liver fibrosis especially caused by HBV [Villeneuve, 2005].

In this work, we purified PM from rat liver fibrosis model, and used a proteomic method to analyze proteins related to liver fibrogenesis. Twenty-two differentially expressed proteins were identified. Of which, ANXA2 was verified to be a potential biomarker of immune liver fibrosis through Western blotting analysis, immunohistochemistry, and ELISA. Further analysis of these proteins provides clues to understand the molecular mechanism of liver fibrosis and offers new biomarkers for non-invasive diagnosis of liver fibrosis. In conclusion, (1) proteins related to liver fibrosis in PM were detected; and (2) a new possible biomarker, ANXA2, for non-invasive diagnosis of liver fibrosis was verified.

EXPERIMENTAL PROCEDURES

ANIMAL TREATMENT

Ninety-six eight-week-old male Sprague–Dawley rats (180–200 g) were purchased from the Center of Laboratory Animals, Shanghai Public Health Clinical Center, Shanghai, China. All of the animal studies were performed following the relevant national legislation and local guidelines. They were performed at the Centre of Laboratory Animals. The animals were housed four per cage in an animal room (temperature: $23 \pm 2^{\circ}C$; relative humidity: $55 \pm 5^{\circ}C$; and 12-h light and 12-h dark cycle) with unlimited access to food and water. The animals were subjected to the experiment after acclimation for 1 week.

The rats were randomly divided into two groups including PS group and controls. The PS group was intraperitoneally (i.p.) injected with 0.5 ml/rat of PS (COSMO BIO Co., Ltd.) twice a week for up to 8 weeks. The controls were i.p. injected with saline in a dose of 0.5 ml/rat. At 2, 4, 6, and 8 weeks, twelve rats of each group were sacrificed by euthanasia method after being starved for 16–18 h. The samples were used for two-dimensional electrophoresis (2-DE) and Western blotting (6 rats for 2-DE experiment and another 6 for western blot).

HUMAN SUBJECTS

Eleven human liver biopsy were used for immunohistochemical analysis, including five samples with liver fibrosis score of 0 (S0), and six with S4 according to the diagnosis standard of ''Proposal of virus hepatitis'' published in 1995. Twenty-five plasma samples from patients with S0-2 and six healthy controls were used for ELISA. Patients followed up at Shanghai Public Health Clinical Center were recruited in this study. All patients were consistent with the diagnostic criteria of chronic hepatitis B (HBV), but were negative for hepatitis C virus (HCV) and human immunodeficiency virus (HIV). The study protocol was approved by the local Ethics Committee, and all patients were given a written informed consent.

HISTOPATHOLOGY

Rat liver tissue was fixed in 4% paraformaldehyde in PBS. Five-micrometer paraffin sections were stained with Masson or hematoxylin and eosin (H&E) staining and subjected to histopathological examination [Gui et al., 2006]. Score 0, normal (no visible fibrosis); score 1, fibrosis present (collagen fiber present that extends from portal triad or central vein to peripheral region); score 2, mild fibrosis (mild collagen fiber present with extension without compartment formation); score 3, moderate fibrosis (moderate collagen fiber present with some pseudo lobe formation); and score 4, severe fibrosis (severe collagen fiber present with thickening of the partial compartments and frequent pseudo lobe formation).

PREPARATION OF RAT LIVER PMs

PMs were purified as described previously [Zhang et al., 2005, 2006b]. Briefly, the pellet after removing the nuclear was ultracentrifuged using sucrose density gradient of 44.0% and 42.3% at 100,000*g* for 2.5 h. The crude PM (CPM) at the top of 42.3% sucrose was collected and washed. The CPM pellets were further ultracentrifuged at the gradients of 44%, 42.8%, 42.3%, 41.8%, 41.0%, 39.0%, and 37.0%. The pure PM (PPM) at the top of 37.0%

sucrose was collected after centrifugation at 100,000*g* for 6 h. After washed by PBS for twice, the pellet was stored at −80°C in storage buffer (40 Mm HEPES, 1 mM PMSF) for Western blotting analysis and proteomic analysis.

TWO-DIMENSIONAL ELECTROPHORESIS (2-DE) AND GEL STAINING

2-DE was performed on an IPGphor isoelectronic focusing system (Amersham Bioscience) and Bio-Rad Protein II electrophoresis apparatus as described previously [Zhang et al., 2006a,b]. About 200 μg of protein from each sample was applied to IPG dry strips (pH 3–10 NL, 180 mm × 30 mm × 0.5 mm). The focusing was performed at 20°C under the following conditions: 30 V for 12 h, 500 V for 1 h, 1,000 V for 1 h, 8,000 V gradient for 30 min, and 8,000 V for 6 h up to 52.1 KVh. About 11.5% separation gels were used and run in Bio-Rad Protein II electrophoresis apparatus. After completion of the second-dimensional electrophoresis, the gels were stained for silver nitrate staining or Coomassie blue as described previously [Zhang et al., 2006b].

IMAGE ACQUISITION AND DATA ANALYSIS

The 2-DE gels were scanned by Imagescaner (Amersham Biosciences, Uppsala, Sweden) in a transmission mode, and the image analysis was conducted with ImageMaster 2D Platinum (Amersham Biosciences). To get the comparable data for quantitative analysis, the individual spot volumes were normalized by dividing their optical density (OD) values by the total OD values of all the spots present in the gel. The relative volume of each spot was used as an index to eliminate the density differences caused by the individual experimental errors. The threshold was defined as the significant change in spot volume was at least twofold upon the comparison of the average gels between the liver fibrosis and the controls.

IDENTIFICATION OF DIFFERENTIALLY EXPRESSED PROTEINS BY MASS SPECTROMETRY

The differentially expressed proteins were analyzed by ESI-MS–MS mass spectrometry. Briefly, spots were excised from silver stained gels. The gel pieces were de-stained and digested with trypsin as described previously [Zhang et al., 2006a]. The peptides in gels pieces were extracted twice with 50% acetonitrile and 0.1% trifluoroacetic acid 16–18 h later. All extract solutions were combined and was dried cool. The dried peptides were diluted with 2% ACN in water with 0.1% TFA and analyzed by ESI-Ion-Trap (Esquire HCT, Bruker, Germany) as described previously [Asamoto et al., 2008]. Briefly, the peptide mixture (5 μl) was directly subjected to a nanoLC–ESI–tandem MS system (Esquire HCT; Bruker Daltonics, Bremen, Germany). Chromatography was performed using an Ultimate 3000 instruments (LC Packings; Dionex, Sunnyvale, CA). The tryptic peptide mixtures were injected onto a C18 μ-precolumn (300 μm id × 5 mm, 5 μm, PepMap™) (LC Packings, Amsterdam, the Netherlands) with a flow rate of 200 μl/min. After desalted by precolumn, the peptides were eluted to a C-18 reversed-phase nanocolumn (75 μm id × 15 cm length, 3 μm, PepMap™) (LC Packings). A flow rate of 300 nl/min was set and the continuous acetonitrile gradient consisting of 4–65% B in 40 min was used (solvent A: 100% water with 0.1% formic acid, solvent B: 80% ACN with 0.1% formic acid). The eluted peptides from the reversed-phase nanocolumn were online injected to a PicoTip emitter nanospray needle (New Objective, Woburn, MA) for real-time ionization and peptide fragmentation on an Esquire HCT ion-trap (Bruker-Daltonics, Bremen, Germany) mass spectrometer. Every 1 s, the instrument cycled through acquisition of a full-scan mass spectrum and five MS/MS spectrum. The software Chromeleon version 6.80 was used to control the whole analytical process.

For database search, search parameters were set as follows: enzyme, trypsin; allowance for up to one missed cleavage peptide; mass tolerance, 1.2 Da for MS and MS/MS mass tolerance, 0.6 Da; fixed modification parameter, carbamoylmethylation (C); variable modification parameters, oxidation (at Met); auto hits allowed (only significant hits were report); and results format as peptide summary report. Proteins were identified on the basis of peptides whose ions score exceeded the threshold, $P < 0.05$, which indicates identification at the 95% confidence level for these matched peptides. The proteins identified by more than four peptides were accepted, without manual check. For proteins identified with less than three peptides were manually inspected. Of which, there must be a peptide with four or more continue y-or b-series ions (e.g., y4, y5, y6, y7).

WESTERN BLOTTING AND DENSITOMETRIC ANALYSIS

Fifty micrograms of total protein extracts were separated by electrophoresis in SDS–11.5% polyacrylamide gel and transferred to PVDF membrane (Millipore). Blots were incubated overnight at 4°C with primary antibodies (mouse anti-Na^+/K^+-ATPase (1:5,000; Abcam, Cambridge, UK), rabbit anti-prohibitin (1:100; Abcam), goat anti-GAPDH (1:500; Santa Cruz, CA), rabbit anti-human annexin 2 (1:4,000, Santa Cruz), and anti-human K8 (1:1,000, Abcam). After three washes with TBS–Tween, blots were incubated for 1 h at 20°C with secondary antibody. The immune complexes were revealed by enhanced chemiluminescence and detected by X-ray films. Finally, the X-ray films were scanned and densitometric analysis was performed using the Bio-Rad Quantity One software. Each reaction was performed in triplicate.

IMMUNOHISTOCHEMISTRY AND SEMI-QUANTITATION OF ANXA2

Immunohistochemistry was performed as described previously [van Gijssel et al., 2002; de Seigneux et al., 2007]. Sections (5 μm) of paraffin-embedded tissues were deparaffinized, hydrated, and washed three times in PBS. Subsequently, the slides were incubated overnight at 4°C with rabbit anti-ANXA2 in a humidified chamber (dilution 1:100). The slides were washed in PBS for three times, incubated with Horseradish Peroxidase-conjugated anti-rabbit antibody, and signals detected using a liquid 3, 3′-diaminobenzidine (DAB) staining kit (Gene Tech), counterstained with hematoxylin–exon, dehydrated, mounted in Permount (Fisher Scientific), and imaged digitally by light microscopy using an Olympus BX40 equipped with a logenE PAS9000.

To semi-quantitatively analyze the expression of ANXA2 in liver tissue, each slide was randomly imaged for 10 times in 400-fold magnification. The ANXA2-positive cells were counted in each image. The ratio of the average number of positive cells from six patients with S4 (total of 60 images) to that of five patients with S0 (total of 50 images) was considered as the change rate of ANXA2 expression.

HBV PURIFICATION AND CELL STIMULATION

HBV were purified from patients' plasma with the concentration of HBV above 10^7 copies/ml through sucrose density gradient centrifugation [Mabit et al., 1994; Kaito et al., 2006]. The purification was detected by scanning electron microscope and quantification was carried using real-time RT-PCR.

Huh7 cells, a differentiated human hepatoma cells, which is widely used in HBV-related research [Zhang et al., 2006c; Thompson et al., 2009; Yang et al., 2009], were grown on microscope slides (10 mm × 10 mm) as a monolayer in Dulbecco's minimal essential medium supplemented with 10% fetal calf serum (FCS), 100 U/ml penicillin, 100 μg/ml streptomycin, 20 mM glucose, and minimal essential medium non-essential amino acids at 37°C and 5% CO_2. Huh7 cells were exposed to HBV (10^5copies/ml Dulbecco's minimal essential medium) for various times (2, 4, 6, and 8 h), and collected at 2, 4, 6, and 8 h after stimulation and used for immunocytochemical analysis. The cells were fixed with 4% paraformaldehyde in PBS and permeabilized with 50% acetone/50% methanol for 30 s. The samples were treated as follows: H_2O_2 permeation for 30 s, 5% BSA blocking for 1 min, anti-ANXA2 incubation for overnight, and second antibody incubation for 1 h, lastly detected by DAB.

ENZYME-LINKED IMMUNOSORBENT ASSAY (ELISA)

Sera were submitted to an ELISA test for detection of ANXA2 using a human ANXA2 ELISA kit (USCN Life Science & Tech Co.) following manufacturer's protocol. A 96-well maxi-sorp microtiter plate was coated with blank and samples at 37°C for 2 h, and incubated with detection reagent A and detection reagent B at 37°C for 1 h in turn, stopped with stop solution, and then determined using a microplate reader set to 450 nm.

RESULTS

HISTOPATHOLOGICAL FINDINGS

As shown in Figure 1, the liver fibrosis model was successfully established. At 2 weeks after injection, inflammatory cell infiltration and hepatic fibrosis occurred slightly around the portal area, and liver fibrosis was diagnosed as S0-1 through Masson staining (Fig. 1), James's staining (Fig. S1), and HE staining (Fig. S2). At 4 weeks, hepatic fibrosis was developed to S2. At 6 weeks, rat liver was separated into thin and small-sized pseudolobules, and was diagnosed as S3-4. At 8 weeks, very obvious pseudolobules were developed, with the character of S4 through Masson staining (Fig. 1), James's staining (Fig. S1), and HE staining (Fig. S2). On the other hand, the liver of the control group showed no histopathological changes during the entire experiment span.

PURIFICATION OF PM

The purity of PM was evaluated by Western blotting (Fig. 2). The results showed that PM was enriched for 149-fold [the signal intensity of Na^+/K^+-ATPase (a PM marker) was 45-fold increase, and that of prohibitin (a Mitochondria marker) was decreased 3.3-fold in PM compared with homogenate] through Quantity One 4.1.0 software (Bio-Rad) analysis.

2-DE PROFILES OF PM OF LIVER FIBROSIS

The PM proteins of ILF (immune liver fibrosis) model and the controls were extracted for 2-DE analysis at 2 and 8 weeks. In the 2-DE analysis, the spots of detectable protein ranged from 500 to 650 on 18-cm 2D gels (pH 3-10NL) loaded with 200-μg PM proteins per gel. No obvious changes were observed in the numbers of spots of detectable protein at different weeks after injection (Fig. 3). On the

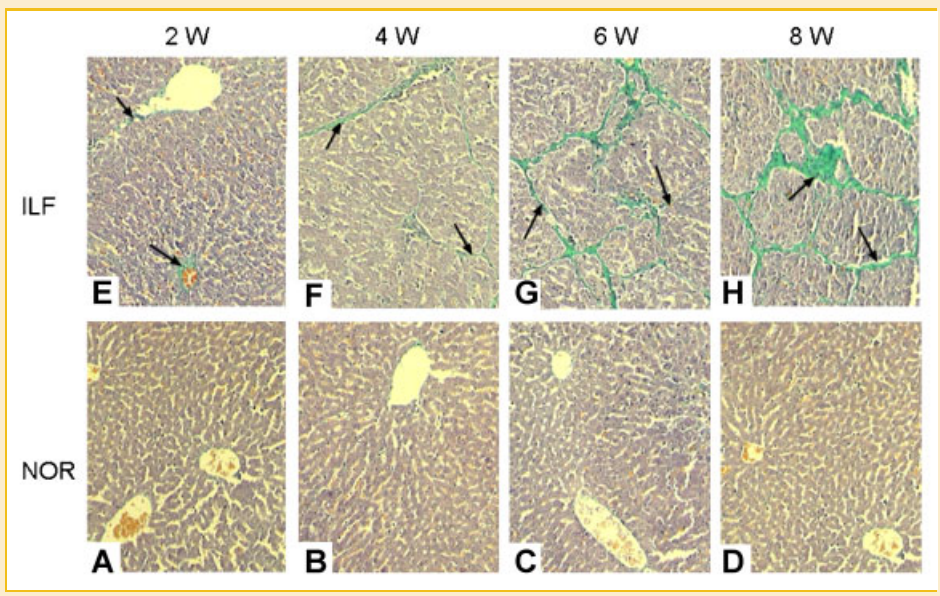

Fig. 1. Histopathology of liver fibrosis examined by Masson staining. NOR (A, B, C, and D), rat livers treated with saline for 2, 4, 6, and 8 weeks (W), and ILF (E, F, G, and H), rat livers treated with PS for 2, 4, 6, and 8 weeks (W), respectively. No obvious difference was found during the growth from 2 to 8 W in normal rats. For ILF model, the degree of liver fibrosis was increased gradually from S0–1 at 2 W, S2 at 4 W, S3–4 at 6 W, to S4 at 8 W as indicated in green and highlighted by arrowhead.

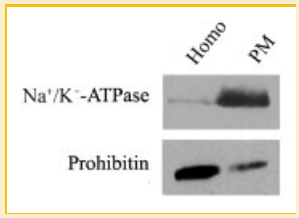

Fig. 2. Verification of PM through Western blotting. The blottings were probed with antibodies against organelle-specific proteins: anti-Na^+/K^+-ATPase for PM; anti-prohibitin for mitochondria. Homo and PM mean homogenization and plasma membrane from rat liver at 4 weeks.

basis of the average intensity ratios of protein spots, a total of 70 protein spots were found to be dynamically changed during the development of liver fibrosis including 26 differential proteins at 2 weeks and 44 at 8 weeks. Among these differential proteins, 14 and 23 proteins were significantly up-regulated at 2 and 8 weeks (ratio ILF/Normal ≥ 2, $P \leq 0.05$), respectively (data not shown).

IDENTIFICATION AND BIOINFORMATICS ANALYSIS OF DIFFERENTIALLY EXPRESSED PROTEINS

20 and 20 protein spots with a threshold greater than twofold were excised from the 2-DE gels at 2 and 8 weeks, respectively, and subjected to in-gel trypsin digestion and subsequent HCT identification. As shown in Table I, Table S1, Figures 3, 9 and 13, differentially expressed spots were successfully identified, including two and eight up-regulated proteins at 2 and 8 weeks, respectively. According to the annotations from UniProt knowledgebase (Swiss-Prot/TrEMBL) and Gene Ontology Database, the identified proteins were located in PM (36%), mitochondrion (19%), cytoplasma (19%), secreted (11%), endoplasmic reticulum (ER) (7%), unknown (4%), and peroxisome (4%) (Fig. S3A). These proteins have functions as following: binding (46%), enzyme (32%), receptor (7%), transport (7%), constructual (4%), and developmental protein (4%) (Table I, Fig. S3B). Among these differential proteins, ANXA2, a protein with location in PM and secreted extracellular space with binding and enzyme function, was found to be gradually increased in ILF from 2 to 8 weeks compared with the controls, and selected for further research. K8, a protein with PM location and binding function, was down-regulated from 2 to 8 weeks, and also selected for further research.

WESTERN BLOTTING VALIDATION

Two proteins––ANXA2 and K8—were selected for Western blotting analysis at 2, 6, and 8 weeks. GAPDH was used as a loading control. As shown in Figure 4, ANXA2 was gradually up-regulated from 2, 6, to 8 weeks, with 11.9- and 17.7-fold increase in that of 6 and 8 weeks compared with that of 2 weeks. Compared with their controls, 0.6-, 5.2-, and 4.1-fold (n = 3) increasement from 2, 6, to 8 weeks was detected in the expression of ANXA2. For K8, 2.4-, 26.4-, to 17.0-fold (n = 3) reduction was detected from 2, 6, to 8 weeks,

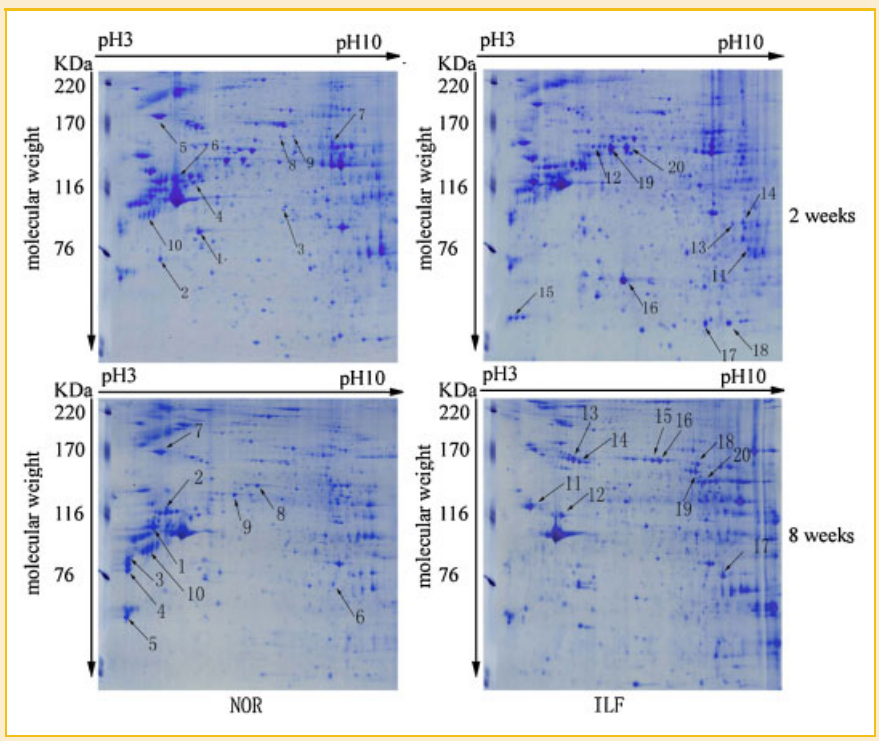

Fig. 3. Protein expression profiles of the ILF and normal control. ILF represents immune liver fibrosis. NOR means healthy control. Two and eight represent the PM at 2 and 8 weeks. The up-regulated protein spots are labeled in the gel of ILF (right); the down-regulated protein spots are marked in the gel of normal (left).

TABLE I. Information of Identified Proteins

Spot	Accession no.	Protein description	Score	pI[a]	MW (KDa)[b]	Cov.[c]	Regulation in model (fold in ILF)	Location	Function
2-1	SPESP_RAT	Sperm equatorial segment protein 1 precursor—*Rattus norvegicus* (Rat)	41	5.06	45.9	1%	0.312	PM	Developmental protein
2-3	CYC_RAT	Cytochrome *c*, somatic—*Rattus norvegicus* (Rat)	77	9.61	11.7	17%	Only in NOR	Mit.	Transport
2-5	TRY1_RAT	Anionic trypsin-1 precursor—*Rattus norvegicus* (Rat)	47	4.71	26.6	8%	0.435	Secreted	Enzyme
2-6	K1C18_RAT	Keratin, type I cytoskeletal 18—*Rattus norvegicus* (Rat)	144	5.17	47.7	29%	0.117	PM	Binding
2-7	CNN1_RAT	Calponin-1—*Rattus norvegicus* (Rat)	33	8.92	33.5	2%	0.239	No	Binding
2-8	TR110_RAT	Taste receptor type 2 member 110—*Rattus norvegicus* (Rat)	40	10.4	38.6	1%	0.368	PM	Receptor
2-10[d]	**K2C8_RAT**	**Keratin, type II cytoskeletal 8—*Rattus norvegicus* (Rat)**	**320**	**5.83**	**54.0**	**35%**	**0.212**	**Cytoplasm**	**Binding**
2-13[d]	**ANXA2_RAT**	**Annexin A2—*Rattus norvegicus* (Rat)**	**205**	**7.55**	**38.9**	**17%**	**2.348**	**PM/secreted**	**Binding**
2-16	NCOAT_RAT	Bifunctional protein NCOAT—*Rattus norvegicus* (Rat)	34	4.04	103.9	3%	6.359	Cytoplasm	Enzyme
8-1, 2, 3, 4	K1C18_RAT	Keratin, type I cytoskeletal 18—*Rattus norvegicus* (Rat)	1,299	5.17	47.7	68%	0.115	PM	Binding
8-6	ARGI1_RAT	Arginase-1—*Rattus norvegicus* (Rat)	331	6.76	35.1	43%	0.185	Cytoplasm	Enzyme
8-7	GRP78_RAT	78 kDa glucose-regulated protein precursor—*Rattus norvegicus* (Rat)	529	5.07	72.4	31%	0.068	ER	Binding
8-8	PDIA3_RAT	Protein disulfide-isomerase A3 precursor—*Rattus norvegicus* (Rat)	301	5.88	57.0	33	Only in NOR	ER	Enzyme
8-10[d]	**K2C8_RAT**	**Keratin, type II cytoskeletal 8—*Rattus norvegicus* (Rat)**	**695**	**5.83**	**54.0**	**41**	**Only in NOR**	**Cytoplasm**	**Binding**
8-11	ATPB_RAT	ATP synthase subunit beta, mitochondrial precursor—*Rattus norvegicus* (Rat)	738	5.19	56.3	53%	14.324	Mit./PM	Binding/enzyme
8-12	QCR1_RAT	Cytochrome b-c1 complex subunit 1, mitochondrial precursor—*Rattus norvegicus* (Rat)	382	5.57	53.5	29%	2.374	Mit.	Enzyme/transport
8-13, 14	ANXA6_RAT	Annexin A6—*Rattus norvegicus* (Rat)	916	7.55	76.1	49%	5.983	Cytoplasm	Binding
8-15	DHSA_RAT	Succinate dehydrogenase [ubiquinone] flavoprotein subunit, mitochondrial precursor—*Rattus norvegicus* (Rat)	366	6.75	72.6	43%	7.348	Mit.	Binding/enzyme
8-16	K2C6A_RAT	Keratin, type II cytoskeletal 6A—*Rattus norvegicus* (Rat)	474	8.06	59.6	11%	3.976	PM	Structural
8-17[d]	**ANXA2_RAT**	**Annexin A2—*Rattus norvegicus* (Rat)**	**313**	**7.55**	**38.9**	**27%**	**4.561**	**PM/secreted**	**Binding**
8-19	ETFD_RAT	Electron transfer flavoprotein–ubiquinone oxidoreductase, mitochondrial precursor—*Rattus norvegicus* (Rat)	155	7.33	69.0	22%	2.168	Mit./PM	Binding/enzyme
8-20	CATA_RAT	Catalase—*Rattus norvegicus* (Rat)	52	7.07	60.1	7%	3.014	Peroxisome/PM	Enzyme/binding

ER, endoplasmic reticulum; PM, plasma membrane; No, not shown; Mito., mitochondrion.
[a]Theoretical PI.
[b]Theoretical molecular weight.
[c]"Cov" stand for "Sequence coverage". Sequence coverage means the ratio of the experimental peptide sequence in an MS experiment matched to theoretical protein sequence.
[d]Proteins selected for further research.

compared with their controls. These data were basically in line with the expression changes shown by the 2-DE analysis.

IMMUNOHISTOCHEMISTRY

Immunohistochemical studies were performed in rat model biopsy at 2, 4, 6, and 8 weeks using ANXA2 antibodies. The immunohistochemical analysis revealed a good correlation between the antibody staining and the proteome expression profiles obtained by 2-DE. At 2 weeks, very little positive signal was detected in rat liver hepatocytes and fibroblasts (Fig. 5A,4). At 6 weeks, positive signal was found in hepatocytes and even stronger in fibroblast (Fig. 5A,5). At 8 weeks, stronger ANXA2 staining was detected (Fig. 5A,6). In contrast, only little positive signal can be detected in hepatocytes from 2 to 8 weeks in the controls (Fig. 5A,1–3).

To verify the result in human, we performed an immunohistochemical study in human liver biopsy with S0 and S4. As shown in Figure 5B, stronger expression was detected in S4 (four lower panels) compared with S0 (four upper panels). When observed in 400-fold magnification (Fig. 5C), much stronger staining of ANXA2 was detected in PMs of hepatocytes (Fig. 5C,2S4) and fibroblasts (Fig. 5C,3S4) in samples with S4 compared with S0 (Fig. 5C,2S0). Statistical analysis showed that the expression of ANXA2 was increased more than threefold in S4 ($n = 6 \times 10$) compared with in S0 ($n = 5 \times 10$) ($P = 0.0001$) (Fig. 5D).

VALIDATION OF POTENTIAL BIOMARKERS USING IMMUNODETECTION

In order to analyze the possible diagnosis value of ANXA2, we performed ELISA to compare the relative abundance of ANXA2 in plasma of 16 individuals having S1-2, with 9 having S0 and 6 healthy volunteers. Consistent with proteomic results, ELISA results showed that the expression of ANXA2 in the plasma of S1-2 is higher than that in S0 (patients with S0 and healthy donors) with the OD value of 0.044 ± 0.13 ($n = 16$) in S1-2, and 0.032 ± 0.008

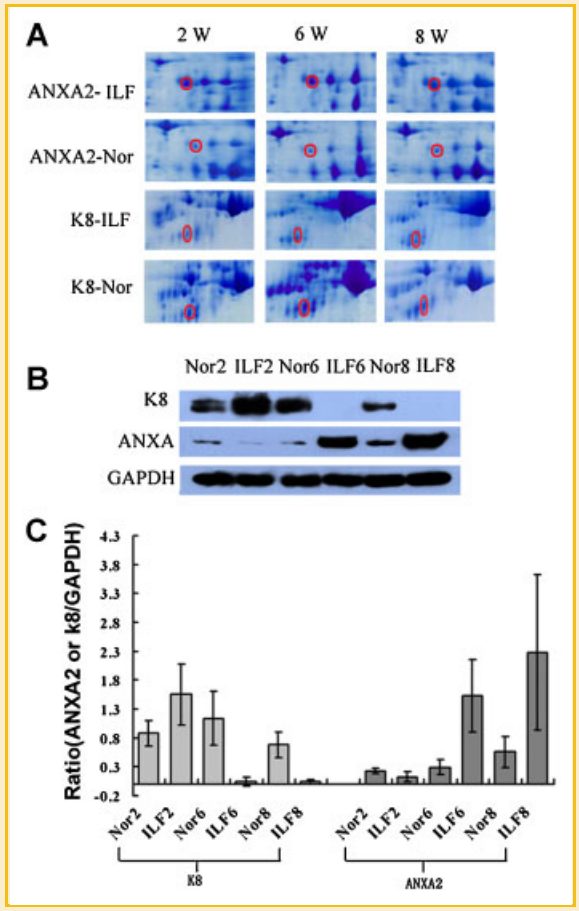

Fig. 4. Western blotting confirmations of representative proteins in ILF and normal control. A: The expression changes of annexin A2 and keratin 8 in 2-DE. B: The expression of annexin A2 and keratin 8 in 2, 6, and 8 weeks rat model. C: The signal intensity of specific bands. The y-axis shows the optical density of protein expression. The data were presented as average value (from a protein loading of 50 μg) and standard deviation (n = 3). *Student's *t*-test; *P*-value <0.05.

(n = 15) in S0. Through paired *t*-test, significant difference ($P = 0.020$) was detected between S1-2 and S0 (Fig. 6). The raw data were shown in Table S2.

EFFECT OF HBV TO ANXA2 IN VITRO

Through sucrose density gradient centrifugation, HBV was enriched with the concentration of 10^9 copies/ml. Electron microscope showed the HBV particles having three kinds of shapes including bar- and granular-type (data not shown). Hepatocyte (Huh7) cells were exposed to HBV for various times (2, 4, 6, and 8 h) to examine the direct effect of HBV to the expression of ANXA2 in vitro. ANXA2 relocation was detected in Huh7 exposed to HBV (Fig. 7). At 2 h, ANXA2 was found mainly in nuclear and cytoplasm, which was observed with the controls. Interesting, when Huh7 cells were exposed to HBV for 4 h, the expression of ANXA2 in nuclear and cytoplasma was markedly decreased while that in PM was greatly increased. By 8 h, most of ANXA2 was found in PM (Fig. 7, HBV-T 8).

DISCUSSION

PROTEOMIC RESEARCH OF LIVER FIBROSIS

As reviewed by Wynn [Wynn, 2007], although a substantial amount of progress has been made over the past few years, a great deal of work is still needed to fully understand the mechanisms of fibrogenesis. Furthermore, the lack of robust biomarkers still limits the evaluation of hepatic fibrosis stages and progression in chronic diseases [Grigorescu, 2006]. To address these needs, proteomics has been widely used to search for new biomarkers [Gangadharan et al., 2007; Spano et al., 2008; Molleken et al., 2009], and understand the mechanisms of fibrosis [Cheung et al., 2008]. Most of these researches focused on the whole cells from serum and liver tissue of human or animal model; however, none have studied the PM proteins. To our knowledge, this study has shown for the first time how PM proteins were affected during the development of ILF in rat model.

RAT MODEL FOR LIVER FIBROSIS

Generally, human liver tissues are more relevant and desirable to study liver fibrosis. However, it is difficult to study proteome related to liver fibrosis using human tissue for the following reasons: (1) dynamically observing the protein changes during fibrogenesis; (2) obtaining enough samples to study PM proteins; and (3) greater individual variance. In this work, ILF rat model was obtained through treating rat with PS. Liver tissues at 2, 4, 6, and 8 weeks were detected to have disease with S0-4. PM proteins from these tissues were extracted and used for proteome research. Differential proteins identified in rat model were verified through immunohistochemical analysis of liver biopsy and ELISA of plasma from patients with liver fibrosis giving the ILF model partially mimicking liver fibrosis in human caused by HBV.

ANXA2 WAS FOUND TO BE RELATED TO LIVER FIBROSIS

In order to identify PM proteins related to liver fibrosis, it is necessary to display the proteins differentially expressed in fibrogenesic liver tissue. According to the report from Pedersen et al. [2003] that 90% of the predicted yeast membrane proteins have a GRAVY value below 0.4, which falls into the solubility range commonly detected on 2D gels. Our previous research [Zhang et al., 2005] also showed PM proteins can be better separated by 2-DE through optimized extraction method. So in this work, we continued to use 2-DE technique to analyze the liver PM proteome during the development of fibrosis. Twenty-two differentially expressed proteins were identified in PM of fibrotic liver. These proteins play important roles in a variety of pathways. From a recent review [Grigorescu, 2006], the differentially expressed proteins identified in this work were not the known biomarkers. In addition to a few proteins that have already been found differentially expressed in animal models or humans of liver injury (such as catalase [Spano et al., 2008], KRT8 and KRT18 [Strnad et al., 2006]), the others were newly found to be related to fibrosis induced by hepatitis B, for example, ANXA2, Calponin-1, and so on.

ANXA2 is a calcium and phospholipid-binding protein. Several molecules known to bind to ANXA2 affect a number of

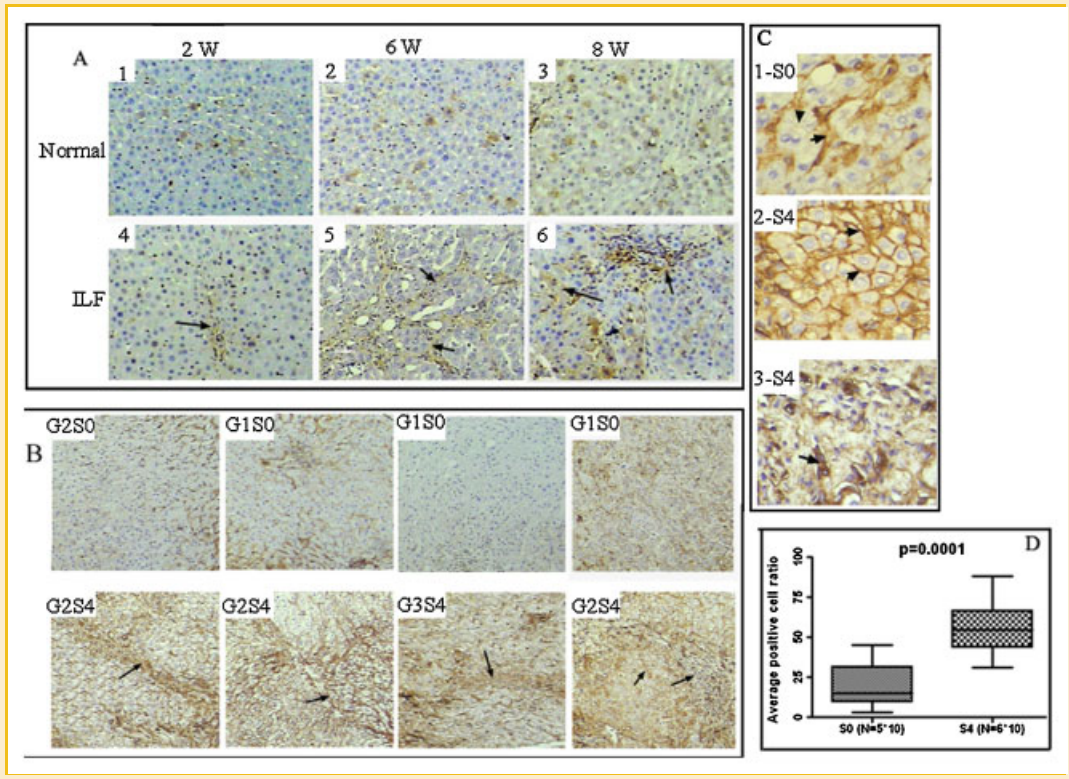

Fig. 5. Immunohistochemistry analysis of annexin A2. A: Immunohistochemistry of rat model (100×): 1, 2, and 3 represent healthy controls at 2, 6, and 8 weeks, respectively, while 4, 5, and 6 represent samples from ILF rats. B: Immunohistochemistry human liver biopsy (100×): top four samples with S0, below four with S4. C: Immunohistochemistry human liver biopsy (400×): 1 with S0, and 2 and 3 with S4. The positive signals are highlighted by arrowheads in (A), (B), and (C). D: Statistical analysis of average annexin A2-positive cell counts. Five patients with S0 and six with S4 were immunohistochemical studies. Each slide from one patient was randomly imaged for 10 times in 400-fold magnification. Significant difference [$P = 0.0001$, S0 ($n = 50$), S4 ($n = 60$)] was detected.

physiologically and pathologically important functions [Brownstein et al., 2004; Gveric et al., 2005]. It has been found to be up-regulated in liver cancer [Mohammad et al., 2008]. There are also researches showing that ANXA2 was up-regulated in alcohol liver fibrosis (ALF) [Seth et al., 2003], and can be directly up-regulated by alcohol [Seth et al., 2008]. Our study showed ANXA2 was also related to liver fibrosis induced by HBV and was a complement to previous studies [Seth et al., 2008]. Considering the gradual development of liver cancer (i.e., from hepatitis to cirrhosis and then liver cancer) caused by virus, this protein might be a potential biomarker for early diagnosis of liver cancer.

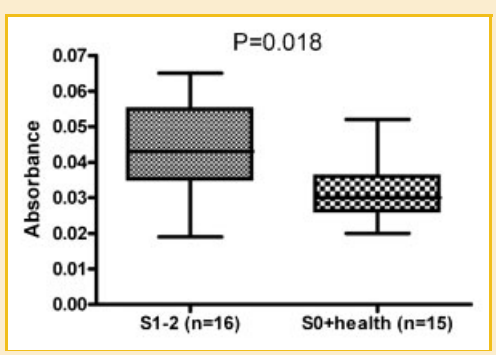

Fig. 6. ELISA analysis of annexin A2 in plasma. Y-axis was the OD values in ELISA. Significant difference ($P = 0.02$) was detected with the value of 0.044 ± 0.13 and 0.032 ± 0.008 in the plasma of S1-2 ($n = 16$) and S0 (patients with S0 and healthy controls) ($n = 15$) through paired-samples *t*-test. annexin A2 was found to be up-regulated for 1.4-fold in liver fibrosis with S1-2 to S0.

EFFECT OF HBV ON THE EXPRESSION OF ANXA2

The driving forces of fibrogenesis include virus (HBV, HCV), alcohol, and so on, Alcohol induced a significant up-regulation of ANXA2 and affected fibrinolysis and plasmin in part through ANXA2 regulation [Seth et al., 2008]. Similarly, our results showed that HBV induced the relocation of ANXA2, and resulted in its up-regulation in PM. This study demonstrates that HBV directly causes the relocation of ANXA2 in PM rather than this altered gene expression being solely a consequence of liver injury itself.

In conclusion, this study provided a subcellular proteome analysis of the difference in hepatocellular PM between liver fibrosis tissues and normal controls using 2-DE–MS that resulted in the identification of a number of proteins related to liver fibrosis. Furthermore, we conclusively demonstrated, for the first time, that ANXA2 is a key protein during the development of immune liver

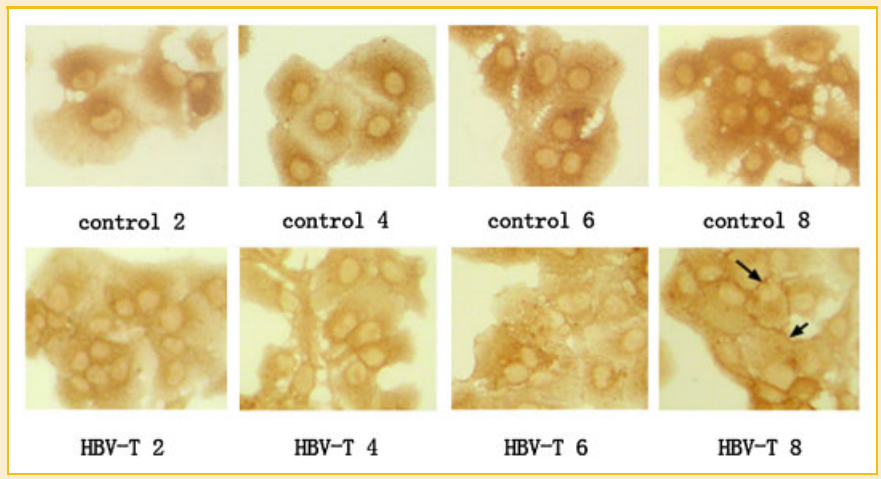

Fig. 7. The relocation of annexin A2 induced by HBV (400×). Control 2, 4, 6, and 8 mean cells stimulated by PBS for 2, 4, 6, and 8 h while HBV-T 2, 4, 6, and 8 for HBV-treated, respectively. Arrows were used to point out the up-regulation of annexin A2 in the plasma membrane of Huh7 cells stimulated by HBV for 8 h.

fibrosis, and has direct relationship with HBV. Collectively, these results suggest that ANXA2 could be a potential biomarker of non-invasive diagnosis of liver fibrosis.

REFERENCES

Asamoto H, Ichibangase T, Uchikura K, Imai K. 2008. Application of an improved proteomics method, fluorogenic derivatization-liquid chromatography-tandem mass spectrometry, to differential analysis of proteins in small regions of mouse brain. J Chromatogr A 1208:147–155.

Baba Y, Uetsuka K, Nakayama H, Dot K. 2004. Rat strain differences in the early stage of porcine-serum-induced hepatic fibrosis. Exp Toxicol Pathol 55:325–330.

Baba Y, Saeki K, Onodera T, Doi K. 2005. Serological and immunohistochemical studies on porcine-serum-induced hepatic fibrosis in rats. Exp Mol Pathol 79:229–235.

Benyon RC, Iredale JP. 2000. Is liver fibrosis reversible? Gut 46:443–446.

Brownstein C, Deora AB, Jacovina AT, Weintraub R, Gertler M, Khan KM, Falcone DJ, Hajjar KA. 2004. Annexin II mediates plasminogen-dependent matrix invasion by human monocytes: Enhanced expression by macrophages. Blood 103:317–324.

Cheung KJ, Tilleman K, Deforce D, Colle I, Van Vlierberghe H. 2008. Proteomics in liver fibrosis is more than meets the eye. Eur J Gastroenterol Hepatol 20:450–464.

Chisari FV, Ferrari C. 1995. Hepatitis B virus immunopathology. Springer Semin Immunopathol 17:261–281.

de Laurentiis A, Donovan L, Arcaro A. 2007. Lipid rafts and caveolae in signaling by growth factor receptors. Open Biochem J 1:12–32.

de Seigneux S, Malte H, Dimke H, Frokiaer J, Nielsen S, Frische S. 2007. Renal compensation to chronic hypoxic hypercapnia: Downregulation of pendrin and adaptation of the proximal tubule. Am J Physiol Renal Physiol 292: F1256–F1266.

Fujisawa G, Muto S, Okada K, Kusano E, Ishibashi S. 2006. Mineralocorticoid receptor antagonist spironolactone prevents pig serum-induced hepatic fibrosis in rats. Transl Res 148:149–156.

Gangadharan B, Antrobus R, Dwek RA, Zitzmann N. 2007. Novel serum biomarker candidates for liver fibrosis in hepatitis C patients. Clin Chem 53:1792–1799.

Gressner OA, Weiskirchen R, Gressner AM. 2007. Biomarkers of liver fibrosis: Clinical translation of molecular pathogenesis or based on liver-dependent malfunction tests. Clin Chim Acta 381:107–113.

Grigorescu M. 2006. Noninvasive biochemical markers of liver fibrosis. J Gastrointestin Liver Dis 15:149–159.

Gui SY, Wei W, Wang H, Wu L, Sun WY, Chen WB, Wu CY. 2006. Effects and mechanisms of crude astragalosides fraction on liver fibrosis in rats. J Ethnopharmacol 103:154–159.

Gveric D, Herrera BM, Cuzner ML. 2005. tPA receptors and the fibrinolytic response in multiple sclerosis lesions. Am J Pathol 166:1143–1151.

Kaito M, Ishida S, Tanaka H, Horiike S, Fujita N, Adachi Y, Kohara M, Konishi M, Watanabe S. 2006. Morphology of hepatitis C and hepatitis B virus particles as detected by immunogold electron microscopy. Med Mol Morphol 39:63–71.

Liaw YF. 2009. Natural history of chronic hepatitis B virus infection and long-term outcome under treatment. Liver Int 29(Suppl. 1):100–107.

Liu Y, He J, Ji S, Wang Q, Pu H, Jiang T, Meng L, Yang X, Ji J. 2008. Comparative studies of early liver dysfunction in senescence-accelerated mouse using mitochondrial proteomics approaches. Mol Cell Proteomics 7:1737–1747.

Mabit H, Dubanchet S, Capel F, Dauguet C, Petit MA. 1994. In vitro infection of human hepatoma cells (HepG2) with hepatitis B virus (HBV): Spontaneous selection of a stable HBV surface antigen-producing HepG2 cell line containing integrated HBV DNA sequences. J Gen Virol 75(Pt 10):2681–2689.

Mannova P, Fang R, Wang H, Deng B, McIntosh MW, Hanash SM, Beretta L. 2006. Modification of host lipid raft proteome upon hepatitis C virus replication. Mol Cell Proteomics 5:2319–2325.

Mohammad HS, Kurokohchi K, Yoneyama H, Tokuda M, Morishita A, Jian G, Shi L, Murota M, Tani J, Kato K, Miyoshi H, Deguchi A, Himoto T, Usuki H, Wakabayashi H, Izuishi K, Suzuki Y, Iwama H, Deguchi K, Uchida N, Sabet EA, Arafa UA, Hassan AT, El-Sayed AA, Masaki T. 2008. Annexin A2 expression and phosphorylation are up-regulated in hepatocellular carcinoma. Int J Oncol 33:1157–1163.

Molleken C, Sitek B, Henkel C, Poschmann G, Sipos B, Wiese S, Warscheid B, Broelsch C, Reiser M, Friedman SL, Tornoe I, Schlosser A, Kloppel G, Schmiegel W, Meyer HE, Holmskov U, Stuhler K. 2009. Detection of novel biomarkers of liver cirrhosis by proteomic analysis. Hepatology 49:1257–1266.

Pedersen SK, Harry JL, Sebastian L, Baker J, Traini MD, McCarthy JT, Manoharan A, Wilkins MR, Gooley AA, Righetti PG, Packer NH, Williams

KL, Herbert BR. 2003. Unseen proteome: Mining below the tip of the iceberg to find low abundance and membrane proteins. J Proteome Res 2:303–311.

Pizarro-Cerda J, Cossart P. 2006. Bacterial adhesion and entry into host cells. Cell 124:715–727.

Pungpapong S, Kim WR, Poterucha JJ. 2007. Natural history of hepatitis B virus infection: An update for clinicians. Mayo Clin Proc 82:967–975.

Schuppan D, Ruehl M, Somasundaram R, Hahn EG. 2001. Matrix as a modulator of hepatic fibrogenesis. Semin Liver Dis 21:351–372.

Seth D, Leo MA, McGuinness PH, Lieber CS, Brennan Y, Williams R, Wang XM, McCaughan GW, Gorrell MD, Haber PS. 2003. Gene expression profiling of alcoholic liver disease in the baboon (*Papio hamadryas*) and human liver. Am J Pathol 163:2303–2317.

Seth D, Hogg PJ, Gorrell MD, McCaughan GW, Haber PS. 2008. Direct effects of alcohol on hepatic fibrinolytic balance: Implications for alcoholic liver disease. J Hepatol 48:614–627.

Smyth R, Lane CS, Ashiq R, Turton JA, Clarke CJ, Dare TO, York MJ, Griffiths W, Munday MR. 2009. Proteomic investigation of urinary markers of carbon-tetrachloride-induced hepatic fibrosis in the Hanover Wistar rat. Cell Biol Toxicol.

Spano D, Cimmino F, Capasso M, D'Angelo F, Zambrano N, Terracciano L, Iolascon A. 2008. Changes of the hepatic proteome in hepatitis B-infected mouse model at early stages of fibrosis. J Proteome Res 7:2642–2653.

Strnad P, Lienau TC, Tao GZ, Lazzeroni LC, Stickel F, Schuppan D, Omary MB. 2006. Keratin variants associate with progression of fibrosis during chronic hepatitis C infection. Hepatology 43:1354–1363.

Thompson AJ, Colledge D, Rodgers S, Wilson R, Revill P, Desmond P, Mansell A, Visvanathan K, Locarnini S. 2009. Stimulation of the interleukin-1 receptor and Toll-like receptor 2 inhibits hepatitis B virus replication in hepatoma cell lines in vitro. Antivir Ther 14:797–808.

Tsukamoto H, Matsuoka M, French SW. 1990. Experimental models of hepatic fibrosis: A review. Semin Liver Dis 10:56–65.

van Gijssel HE, Divi RL, Olivero OA, Roth MJ, Wang GQ, Dawsey SM, Albert PS, Qiao YL, Taylor PR, Dong ZW, Schrager JA, Kleiner DE, Poirier MC. 2002. Semiquantitation of polycyclic aromatic hydrocarbon-DNA adducts in human esophagus by immunohistochemistry and the automated cellular imaging system. Cancer Epidemiol Biomarkers Prev 11:1622–1629.

Villeneuve JP. 2005. The natural history of chronic hepatitis B virus infection. J Clin Virol 34(Suppl. 1):S139–S142.

Wang K, Fan X, Fan Y, Wang B, Han L, Hou Y. 2007. Study on the function of circulating plasmacytoid dendritic cells in the immunoactive phase of patients with chronic genotype B and C HBV infection. J Viral Hepat 14: 276–282.

Wynn TA. 2007. Common and unique mechanisms regulate fibrosis in various fibroproliferative diseases. J Clin Invest 117:524–529.

Yang JC, Teng CF, Wu HC, Tsai HW, Chuang HC, Tsai TF, Hsu YH, Huang W, Wu LW, Su IJ. 2009. Enhanced expression of vascular endothelial growth factor-A in ground glass hepatocytes and its implication in hepatitis B virus hepatocarcinogenesis. Hepatology 49:1962–1971.

Zhang L, Xie J, Wang X, Liu X, Tang X, Cao R, Hu W, Nie S, Fan C, Liang S. 2005. Proteomic analysis of mouse liver plasma membrane: Use of differential extraction to enrich hydrophobic membrane proteins. Proteomics 5:4510–4524.

Zhang L, Liu X, Zhang J, Cao R, Lin Y, Xie J, Chen P, Sun Y, Li D, Liang S. 2006a. Proteome analysis of combined effects of androgen and estrogen on the mouse mammary gland. Proteomics 6:487–497.

Zhang LJ, Wang XE, Peng X, Wei YJ, Cao R, Liu Z, Xiong JX, Yin XF, Ping C, Liang S. 2006b. Proteomic analysis of low-abundant integral plasma membrane proteins based on gels. Cell Mol Life Sci 63:1790–1804.

Zhang XN, Liu JX, Hu YW, Chen H, Yuan ZH. 2006c. Hyper-activated IRF-1 and STAT1 contribute to enhanced interferon stimulated gene (ISG) expression by interferon alpha and gamma co-treatment in human hepatoma cells. Biochim Biophys Acta 1759:417–425.